

Dual-energy contrast-enhanced CT to evaluate Scaphoid Osteonecrosis with surgical correlation

Pianta M (1)\*, McCombe D (2), Slavin J (3), Hendry S (3), Perera W (1)

Marcus Pianta (corresponding author, Department of Medical Imaging)

David McCombe (Department of Surgery)

John Slavin (Department of Anatomical Pathology)

Shona Hendry (Department of Anatomical Pathology)

Warren Perera (Department of Medical Imaging)

St Vincent's Hospital

Fitzroy, Victoria, Australia 3065

[marcus.pianta@svha.org.au](mailto:marcus.pianta@svha.org.au)

+613-9288-4310

This is the author manuscript accepted for publication and has undergone full peer review but has not been through the copyediting, typesetting, pagination and proofreading process, which may lead to differences between this version and the [Version of Record](#). Please cite this article as [doi: 10.1111/1754-9485.12796](https://doi.org/10.1111/1754-9485.12796)

This article is protected by copyright. All rights reserved

1  
2  
3  
4  
5  
6  
7  
8  
9  
10  
11  
12  
13  
14  
15  
16  
17  
18  
19  
20  
21  
22  
23  
24  
25  
26  
27  
28  
29  
30  
31  
32  
33

DR. MARCUS PIANTA (Orcid ID : 0000-0001-5015-3361)

Article type : Radiology Technical Article

**Abstract:**

Objective, To evaluate the validity of contrast enhanced dual energy CT using a lung perfusion algorithm in assessing for post-traumatic scaphoid proximal pole avascular necrosis.

Materials and Methods, From Aug 2013 to Aug 2016, 18 patients (19 wrists, 16 males, 2 females, mean age 28 years) were assessed as high-risk for proximal pole scaphoid avascular necrosis by a single surgeon following a scaphoid fracture and were referred for contrast-enhanced dual energy CT. 8 wrists had specimens sent for correlative histological analysis and 11 were correlated with operative notes.

Results, 8 surgical specimens were sent to histology and showed a 100% correlation (8/8) with the DECT findings. The remaining 11 wrists that did not have a specimen sent had in-surgery findings that also correlated with DECT. A single case was discrepant (1/11) due to presence of an intra-osseous ganglion, which was reported as osteonecrosis on CT, but considered viable at surgery. No case was called viable on CT that proved to be necrotic at either surgery or histologically.

Conclusion, Contrast-enhanced dual energy CT using a perfusion algorithm is an innovative and promising method in evaluating viability of the post-trauma proximal pole of scaphoid.

**Keywords:**

computed tomography; dual energy; osteonecrosis; perfusion; scaphoid; vascularity

**Introduction:**

34 It is crucial to identify avascular necrosis of the proximal pole fragment in scaphoid  
35 fractures given the implications of impaired fragment vascularity for management and  
36 prognosis (1).

37

38 The predominant scaphoid blood supply enters the scaphoid distally via the dorsal  
39 ridge of the scaphoid, and a fracture of the waist or proximal scaphoid leaves the  
40 proximal pole susceptible to avascular necrosis (AVN) given this will disrupt the  
41 intraosseous vessels. Impaired vascularity of the proximal fragment contributes to a  
42 greater risk of nonunion (1,2). The reference standard for assessing vascularity of the  
43 proximal scaphoid pole in treating nonunited fractures is direct assessment of the  
44 degree of intraoperative bleeding from the cancellous bone of the proximal pole  
45 fragment (3).

46 Whilst MRI is an excellent modality for assessing a scaphoid fracture as well as  
47 associated cartilage and ligamentous damage, it can also help evaluate vascularity and  
48 integrity of the proximal pole (2). Problems with MRI include access, economic cost,  
49 extended time to complete the study, contraindications such as some pacemakers or  
50 cochlear implants, patient claustrophobia and allergy to contrast dye (gadolinium).  
51 Many of these can be addressed with use of Computed Tomography (CT), but  
52 traditionally this has not provided adequate information about proximal pole  
53 vascularity.

54 Computed Tomography can reveal more detail than plain radiographs which are often  
55 performed at the time of initial injury (3). CT can identify an occult fracture and  
56 better demonstrate fracture anatomy and assist in treatment planning in cases where  
57 there is ongoing pain despite good early healing or where there is some complication  
58 such as comminution, displacement, intra-articular step and suspected cartilage  
59 damage. Determining the anatomy of the fracture, particularly whether of the  
60 scaphoid waist compared to a proximal pole is also important given the improved  
61 surgical outcomes for the former (4).

62

63 Dual Energy CT is a scan technique that utilises differences in material atomic  
64 number, assessed with 2 beams of ionizing radiation at different energies (kVp). In  
65 musculoskeletal imaging, this has been used to good effect in assessing gout, metal  
66 artifact reduction and bone bruising (5). In thoracic imaging, CT perfusion can be  
67 performed of the lungs in cases of suspected pulmonary embolus (6), whereby an

68 iodine map is generated on a post-contrast study using values of air, soft tissue and  
69 contrast medium ratio. In this way regions of lung parenchyma can be assessed for  
70 decreased iodine uptake ('contrast enhancement'), which can indicate more proximal  
71 vascular arterial occlusion. We have adapted this technique to assess scaphoid  
72 vascularity.

73  
74 The objective of our pilot study is to correlate post-contrast Dual energy CT using a  
75 lung perfusion-algorithm in suspected post traumatic scaphoid proximal pole AVN  
76 with surgery and histology.

### 77 78 79 **Materials and Methods:**

80 Institutional Review Board ethics approval was obtained for this retrospective review  
81 study. All patients with a scaphoid fracture and clinical concern for proximal pole  
82 avascular necrosis (AVN) from August 2013 to August 2016 who were referred to a  
83 hand surgeon and had undergone DECT were considered for the study (54 patients, 55  
84 wrists). 36 patients were excluded due to being considered at a 'lower-risk' by the  
85 surgeon. A total of 18 patients (19 wrists, 2 females and 16 males, age range 15 – 61  
86 years, mean 28, median 24) were included and of these, 8 wrists underwent surgery  
87 with surgical specimens sent for histopathological correlation (approximately 0.2-0.4  
88 cc<sup>3</sup> fragments of bone). 11 wrists underwent DECT and correlation with operative  
89 notes without histology specimen sent. Those with multiple DECT scans had all  
90 included in the analysis (single patient, one CT scan each wrist).

91  
92 Patients were scanned following intravenous contrast administration (75 cc  
93 Omnipaque-370 (GE Healthcare, Princeton, New Jersey) 90 second delay) at dual  
94 energy on a Siemens Somatom Force CT scanner (Siemens AG, Erlangen, Germany).  
95 One wrist was scanned per field of view. Post processing was performed on the  
96 Syngo.Via workstation, version 2.0 VA30A, (Siemens Healthcare, Erlangen,  
97 Germany) and images sent to PACS. All scans were read by 2 fellowship trained  
98 musculoskeletal radiologists independently who had some limited experience with  
99 interpretation of cases including surgical correlation, performed prior to this study.

100

101 The patient's dual energy CT scan data was loaded into Syngo via. The chest – pooled  
102 blood volume algorithm was selected with the default settings and then the maximum  
103 Hounsfield unit (HU) was changed from -600 to +500 in order to increase the  
104 threshold of displayed densities such as contrast-enhancing material in dense bone,  
105 including the scaphoid which has a Hounsfield unit of approximately 500.(7, 8) This  
106 also enabled generation of visible and assessable colour maps which were stored for  
107 reference on PACS. These images were then correlated with a) intra-operative  
108 assessment of AVN (relating to proximal pole bleeding with probing during surgery)  
109 and/or b) a histological specimen of the cancellous bone that was curetted from the  
110 proximal pole fragment as part of preparation of the surface of the fragment for bone  
111 grafting and fixation of the fracture.

112

113 Criteria for radiologic AVN was strictly defined by the colour map distribution output  
114 from Syngo.Via. Results were recorded as either viable or necrotic. If the proximal  
115 pole demonstrated similar colour as the more distal scaphoid, it was considered  
116 viable. If it predominantly (Reader impression of >50% whilst scrolling through  
117 coronal colour map images) had no colour, it was recorded as necrotic. Changes in  
118 proximal pole density or bone mineralisation were not considered for this study.  
119 Excluded patients included those with significant wrist or hand metalware that  
120 resulted in distortion of the colour map due to artifact.

121

122

### 123 **Results:**

124 Of the 19 wrists with a scaphoid fracture which were reviewed by a specialist hand  
125 surgeon and underwent DECT, 8 were clinically assessed as being at a higher  
126 suspicion for AVN and underwent surgery with specimens sent to pathology (Table  
127 1). The other 11 of the 19 surgical wrists had DECT performed without a histological  
128 specimen sent, and correlation was made with operative notes as to scaphoid fracture  
129 site bleeding status.

130

131 Table 1.

132

133 All 8 surgical specimens correlated with the DECT findings. 6 no AVN (Figure 1)  
134 and 2 AVN (Figure 2 & 4). All cases were treated surgically with open reduction and

135 internal fixation (ORIF) with either vascularised or non-vascularised bone graft  
136 obtained from the distal radius or in one case a non-vascularised graft from the iliac  
137 crest.

138

139 Of the 11 DECT scans performed of wrists which did not have a surgical specimen  
140 evaluated but were correlated with the operative report, only a single case of DECT  
141 suggested AVN but at surgery the scaphoid was considered viable with a large intra-  
142 osseous ganglion within the proximal pole accounting for the erroneous CT findings  
143 (Figure 3). There was no instance where the DECT suggested viability (no AVN) and  
144 at surgery found to be osteonecrosis (Table 2).

145

146 Table 2.

147

148 Considering the total 19 wrists that underwent surgery, DECT demonstrates a  
149 sensitivity of 100% (95% CI: 16-100%) and specificity of 94% (71.3-99.9%) for  
150 detecting proximal pole necrosis in cases of scaphoid fracture.

151

152 Viable proximal scaphoid

153

154 Figure 1a, b & c.

155

156

157 Non-perfusion of the proximal pole compatible with osteonecrosis

158

159 Figure 2a, b & c

160

161

162 Large intraosseous cyst of the proximal pole with heterogeneous perfusion.

163

164 Figure 3a, b & c

165

166

167 Patchy uptake of a proximal pole <50% with sclerosis compatible with AVN.

168

169 Figure 4a, b & c

170

171

172 **Discussion:**

173 Whilst musculoskeletal imaging has benefited from the use of dual energy CT scans  
174 in assessing for gout, metal artifact reduction and bone mineral density amongst  
175 others, assessing perfusion in bone has traditionally been the domain of MRI using a  
176 gadolinium contrast agent to assess for uptake in bone, often observed over a time  
177 period or delay (9), or a nuclear medicine Technetium-99m bone scan. There has been  
178 no data on assessing bone viability with contrast enhanced dual energy CT, although  
179 measuring Hounsfield units in the proximal pole has been studied (10) without  
180 showing a reliable correlation.

181

182 Following acquisition of a contrast-enhanced Dual-Energy CT scan, the Syngo.via  
183 software uses a decomposition algorithm to create an iodine distribution map which  
184 analyses the presence of soft tissue, air and iodinated contrast in tissue including  
185 bone, to generate a colour map essentially of contrast enhancement (perfusion),  
186 overlaid on the scanned anatomy. This process is predominantly automated by the  
187 proprietary Syngo.Via software which evaluates the ratio of air and soft tissue in a  
188 voxel with Hounsfield unit thresholds for each of these at both 80kVp and 140kVp,  
189 whilst deriving the iodine component from the CT numbers at both energy levels. A  
190 Relative Contrast Material parameter of 2.0 indicates iodine attenuation at the 80kVp  
191 setting is twice that of 140kVp, enabling it to be discerned and demonstrated on the  
192 perfusion / colour map, as opposed to completely removing the iodine in so called  
193 “virtual non-contrast” (VNC) images.(11) Whilst useful in cases of suspected  
194 pulmonary embolism where there is a proximal arterial thrombus and reduced iodine  
195 perfusion through the more distal lung parenchyma, the same algorithm has been used  
196 to evaluate perfusion of iodinated contrast-enhancing metastasis in bone(12) and  
197 could theoretically help assess proximal scaphoid pole vascularity that may appear at  
198 risk for AVN. The idea for this study was generated following a vendor demonstration  
199 of an iodine perfusion map in a case of pulmonary embolism, whereby the technique  
200 seemed transferable to the common and difficult problem of post traumatic  
201 osteonecrosis of the scaphoid proximal pole.

202

203 The Dual Energy nature of the CT scan assesses atomic number of the materials in the  
204 field of view i.e. tissue and air. Iodinated material can therefore be analyzed and when  
205 absent, or relatively less in the proximal pole compared to the remainder of the  
206 scaphoid, suggests AVN. The scan can take less than 5 minutes to perform, the actual  
207 image acquisition close to 10 seconds so that temporal resolution is excellent and far  
208 exceeds that of MRI. When MRI is requested, intravenous gadolinium contrast may  
209 be administered in order to improve accuracy (13, 14) however more recently there  
210 remains debate about if and how best to perform a post-contrast study (9, 15, 16), and  
211 whilst bone marrow edema signal can be useful in defining a target region of  
212 abnormality, it is of no help in assessing for the presence of AVN (17, 18). A crucial  
213 benefit of MRI however is in assessing the surrounding soft tissues, including  
214 ligaments, tendons and neurovascular structures in the setting of traumatic injury.  
215 MRI gadolinium-based contrast agents also exhibit a lower reaction / hypersensitivity  
216 rate than CT iodinated contrast(19).

217

218 There is a high correlation between what is found on dual energy CT and the  
219 underlying bone pathology. Donati et al (15) describe the difficulties with obtaining a  
220 representative histology specimen due to the heterogeneity of viable and non-viable  
221 bone within a proximal pole sample, which may be expected in a more acute to  
222 subacute setting. This was not a noted problem for our reading Pathologist and whilst  
223 unsubstantiated, could be due to a longer duration between the trauma and surgery in  
224 our patients, allowing for either viability or necrosis to appear as the dominant  
225 feature. The bone sample sent (and its analysis) is also in a way representative of the  
226 method of observing intra-operative scaphoid bleeding from a particular puncture site,  
227 and whilst not perfect, does seem a reasonable surrogate technique. Whilst the  
228 pathology report was dichotomous (the bone was either necrotic or viable), some CT  
229 scans of viable proximal scaphoid poles did demonstrate small regions of absent  
230 iodine uptake. This was not observed in the pathology specimens possibly due to  
231 sampling error (small sample size or temporal heterogeneity of the avascular necrosis  
232 process), or may alternatively reflect small regions of necrosis that subsequently  
233 healed, or of reversible ischemia, and appear of little consequence to the overall  
234 viability of the proximal pole. 100% of cases (8/8) demonstrated the same findings on  
235 DECT as at surgery when specimens were sent for evaluation. DECT was 91%  
236 accurate (10/11) when compared to surgery where the surgeon made an on-table

237 evaluation (and specimens were not sent for histology analysis). The single case that  
238 was incorrectly called AVN on CT showed an intra-osseous ganglion with  
239 surrounding viable bone at surgery. The strict criteria for the study included a binary  
240 response of perfusion or not of the proximal pole, illustrating the need in everyday  
241 practice to review the anatomical imaging simultaneously to avoid such an error.

242

243 Given such small numbers in this pilot study, if larger patient numbers were to be  
244 used there may be issues with reproducibility due to variant timing between contrast  
245 administration and the scan, differential use of the Syngo.Via workstation, variant  
246 thresholding of values such as maximum Hounsfield unit and contrast medium ratio  
247 and use of different dual energy / dual source scanners and other proprietary software.  
248 Our small patient numbers are a significant limitation given that although 2/8 (25%)  
249 surgical specimens correlated with DECT for AVN, this represents only 2/19 (10.5%)  
250 of a patient population considered “high-risk” . Possible bias exists due to the  
251 exposure of the 2 readers to the same limited experience of reading and discussing  
252 only several scans prior to this study, potentially promoting case analysis in a similar  
253 way and thus contributing to comparable results. Results could be more  
254 comprehensive by evaluating whether there had been a single or multiple traumatic  
255 events, duration from injury to imaging, or duration from imaging to surgery.

256 Quantitative techniques in measuring amount of viable or non viable bone (eg. Area  
257 on a central slice or 3D volume) would be advantageous over our methodology of  
258 observing the coronal colour map images and forming an impression of 3D region  
259 involved by osteonecrosis or not. Ideally all patients undergoing surgery would have  
260 specimens sent for histologic review, although unless the entire proximal pole is sent  
261 to histology, some sampling error would be expected given the temporal  
262 heterogeneity of the avascular necrosis process. This may also result in more even  
263 numbers of AVN and viable samples, the discrepancy of 2 AVN to 6 viable cases in  
264 this series possibly due to samples being sent in cases where there was relatively poor  
265 intra-operative bleeding and therefore a higher suspicion for AVN.

266

267 **Conclusion:**

268 This preliminary retrospective study shows dual energy, contrast-enhanced CT to be a  
269 promising technology to aid the evaluation of post-fracture, proximal-pole scaphoid  
270 viability which may help reduce premature osteoarthritis and pain by prompting

271 appropriate management and early intervention if required. CT evaluation for  
272 anatomy can be assessed simultaneously. Further studies with larger patient numbers  
273 and histologic correlation, defining appropriateness criteria for patients to undergo a  
274 DECT scan and refining post-processing techniques may yield improved diagnostic  
275 accuracy.

276

277

278 **Acknowledgements:**

279 Head CT Radiographer Mr. Marvin Lai at St Vincent's Hospital, Melbourne, for  
280 assistance in protocol development and implementation.

281

282 **Disclosures:**

283 None of the Authors have any conflict of interest to disclose.

284

285 **References:**

- 286 1. Barton NJ. The late consequences of scaphoid fractures. J Bone Joint Surg  
287 Br. 2004;86(5):626-30.
- 288 2. Lutsky K. Preoperative magnetic resonance imaging for evaluating  
289 scaphoid nonunion. J Hand Surg Am. 2012;37(11):2383-5.
- 290 3. Smith ML, Bain GI, Chabrel N, Turner P, Carter C, Field J. Using computed  
291 tomography to assist with diagnosis of avascular necrosis complicating chronic  
292 scaphoid nonunion. J Hand Surg Am. 2009;34(6):1037-43.
- 293 4. Kawamura K, Chung KC. Treatment of scaphoid fractures and nonunions. J  
294 Hand Surg Am. 2008;33(6):988-97.
- 295 5. Mallinson PI, Coupal TM, McLaughlin PD, Nicolaou S, Munk PL, Ouellette  
296 HA. Dual-Energy CT for the Musculoskeletal System. Radiology.  
297 2016;281(3):690-707.
- 298 6. Lu GM, Wu SY, Yeh BM, Zhang LJ. Dual-energy computed tomography in  
299 pulmonary embolism. Br J Radiol. 2010;83(992):707-18.
- 300 7. Swanstrom M, Morse K, Lipman J, Hearn K, Carlson M. Variable Bone  
301 Density of Scaphoid: Importance of Subchondral Screw Placement. J Wrist Surg.  
302 2017.

- 303 8. Rhee SH, Baek GH. A correlation exists between subchondral bone  
304 mineral density of the distal radius and systemic bone mineral density. *Clin*  
305 *Orthop Relat Res.* 2012;470(6):1682-9.
- 306 9. Larribe M, Gay A, Freire V, Bouvier C, Chagnaud C, Souteyrand P.  
307 Usefulness of dynamic contrast-enhanced MRI in the evaluation of the viability of  
308 acute scaphoid fracture. *Skeletal Radiol.* 2014;43(12):1697-703.
- 309 10. Bervian MR, Ribak S, Livani B. Scaphoid fracture nonunion: correlation of  
310 radiographic imaging, proximal fragment histologic viability evaluation, and  
311 estimation of viability at surgery: diagnosis of scaphoid pseudarthrosis. *Int*  
312 *Orthop.* 2015;39(1):67-72.
- 313 11. Kang MJ, Park CM, Lee CH, Goo JM, Lee HJ. Dual-energy CT: clinical  
314 applications in various pulmonary diseases. *Radiographics.* 2010;30(3):685-98.
- 315 12. Lee YH, Kim S, Lim D, Suh JS, Song HT. Spectral parametric segmentation  
316 of contrast-enhanced dual-energy CT to detect bone metastasis: feasibility  
317 sensitivity study using whole-body bone scintigraphy. *Acta Radiol.*  
318 2015;56(4):458-64.
- 319 13. Cerezal L, Abascal F, Canga A, Garcia-Valtuille R, Bustamante M, del Pinal  
320 F. Usefulness of gadolinium-enhanced MR imaging in the evaluation of the  
321 vascularity of scaphoid nonunions. *AJR Am J Roentgenol.* 2000;174(1):141-9.
- 322 14. Muller GM, Mansson S, Muller MF, Ekberg O, Bjorkman A. Assessment of  
323 perfusion in normal carpal bones with dynamic gadolinium-enhanced MRI at 3  
324 Tesla. *J Magn Reson Imaging.* 2013;38(1):168-72.
- 325 15. Donati OF, Zanetti M, Nagy L, Bode B, Schweizer A, Pfirrmann CW. Is  
326 dynamic gadolinium enhancement needed in MR imaging for the preoperative  
327 assessment of scaphoidal viability in patients with scaphoid nonunion?  
328 *Radiology.* 2011;260(3):808-16.
- 329 16. Ng AW, Griffith JF, Taljanovic MS, Li A, Tse WL, Ho PC. Is dynamic  
330 contrast-enhanced MRI useful for assessing proximal fragment vascularity in  
331 scaphoid fracture delayed and non-union? *Skeletal Radiol.* 2013;42(7):983-92.
- 332 17. Schmitt R, Christopoulos G, Wagner M, Krimmer H, Fodor S, van  
333 Schoonhoven J, et al. Avascular necrosis (AVN) of the proximal fragment in  
334 scaphoid nonunion: is intravenous contrast agent necessary in MRI? *Eur J Radiol.*  
335 2011;77(2):222-7.

336 18. Fox MG, Gaskin CM, Chhabra AB, Anderson MW. Assessment of scaphoid  
337 viability with MRI: a reassessment of findings on unenhanced MR images. AJR  
338 Am J Roentgenol. 2010;195(4):W281-6.  
339 19. ACR Manual on Contrast Media [press release].  
340 [https://www.acr.org/~media/ACR/Documents/PDF/QualitySafety/Resources](https://www.acr.org/~media/ACR/Documents/PDF/QualitySafety/Resources/Contrast-Manual/Contrast_Media.pdf/-page=282017)  
341 [/Contrast-Manual/Contrast\\_Media.pdf/ - page=282017](https://www.acr.org/~media/ACR/Documents/PDF/QualitySafety/Resources/Contrast-Manual/Contrast_Media.pdf/-page=282017).

342  
343

344 **Figures:**

345 Figure 1a. Coronal CT Bone algorithm demonstrates a sclerotic-rimmed transverse  
346 scaphoid waist fracture in a 47 year old female. 1b. 3d perfusion render demonstrates  
347 clear iodine uptake of both the proximal and distal scaphoid i.e. Viability and no  
348 osteonecrosis. 1c. H&E stain shows a viable trabecula with osteocytes present in  
349 lacunae (white arrow) and viable adipose tissue in the marrow space.

350

351 Figure 2a. Multiplanar CT perfusion imaging shows absence of iodine uptake of the  
352 proximal scaphoid pole with a transverse waist fracture, in keeping with osteonecrosis  
353 in an 18 year old male. 2b. 3d render with distal scaphoid appearing similar to the  
354 remainder of the carpus and minimal iodine uptake within the proximal pole. 2c. H&E  
355 stain shows a fragment of necrotic bone demonstrating empty lacunae (black closed  
356 arrow) and undergoing resorption by osteoclasts (black open arrow).

357

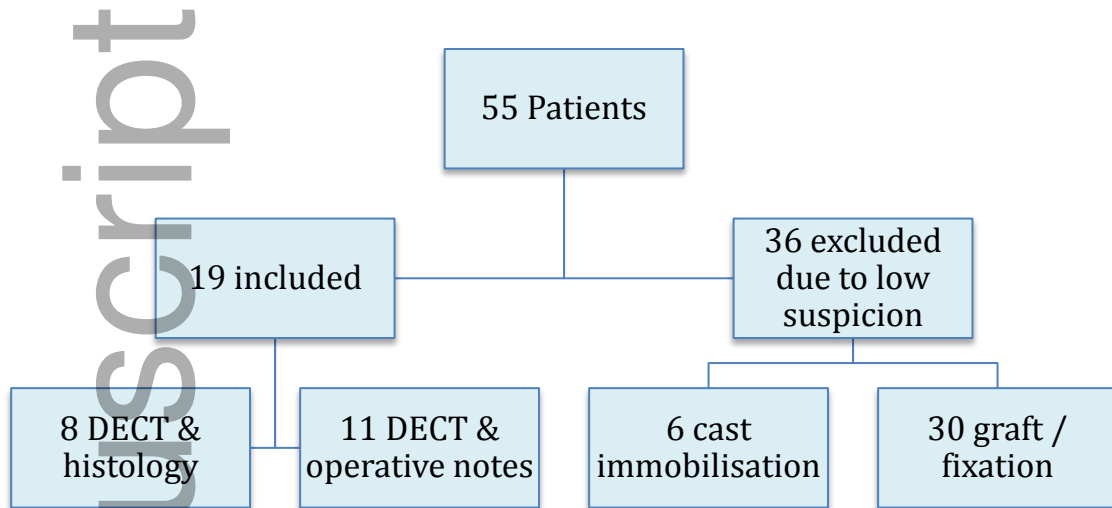
358 Figure 3a. Coronal CT bone algorithm anatomically demonstrates a large intraosseous  
359 cyst of the proximal scaphoid in a 22 year old male. 3b. Coronal fused and 3c. 3D  
360 rendered perfusion imaging demonstrates no iodine uptake in this region –  
361 erroneously reported as osteonecrosis, but viable at surgery.

362

363 Figure 4a. Coronal CT iodine colour distribution map in a 30yo male patient shows  
364 heterogeneous, patchy uptake in the proximal pole but this is less than 50% the  
365 overall volume on the 3D perfusion colour map 4b. which confirms very limited  
366 uptake in the proximal scaphoid and 4c. Coronal bone algorithm CT with transverse  
367 fracture at the junction of proximal and middle thirds with sclerotic proximal pole  
368 typical for osteonecrosis.

369

370 **Tables:**



371

372 **Table 1. Patient group population flowchart.**

373

374

375

	Total Surgery	Total DECT
Total Number	19	19
Viable / Intra-op bleed	9	8
Necrosis / No bleed	10	11

376

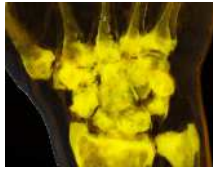
377 **Table 2. Total numbers for Surgery and Dual Energy CT viable and necrotic**  
378 **proximal scaphoid pole.**

# Author Manuscript

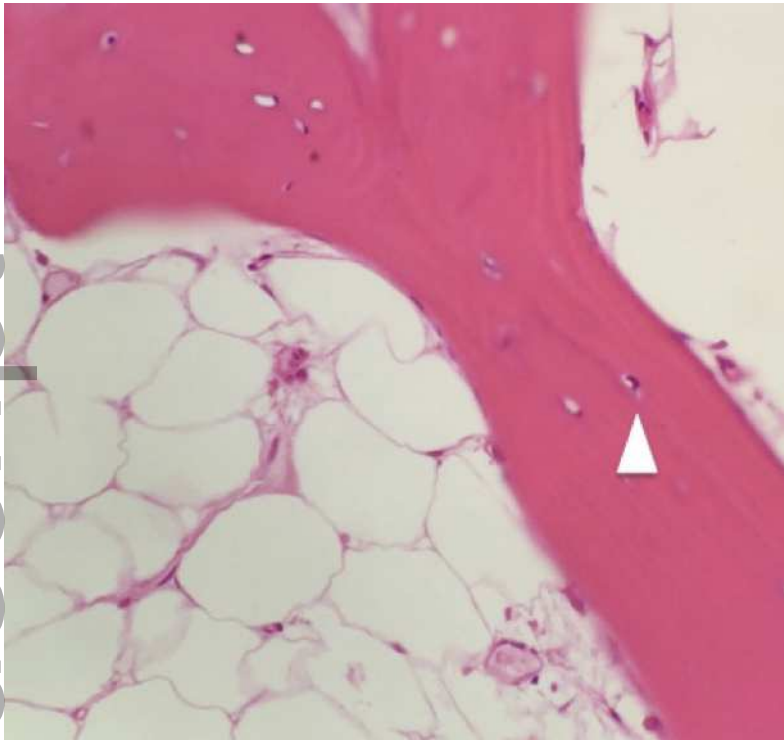


ara\_12796\_f1a.tiff

# Author Manuscript



ara\_12796\_f1b.tiff



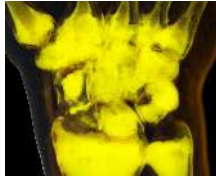
ara\_12796\_f1c.tiff

# Author Manuscript

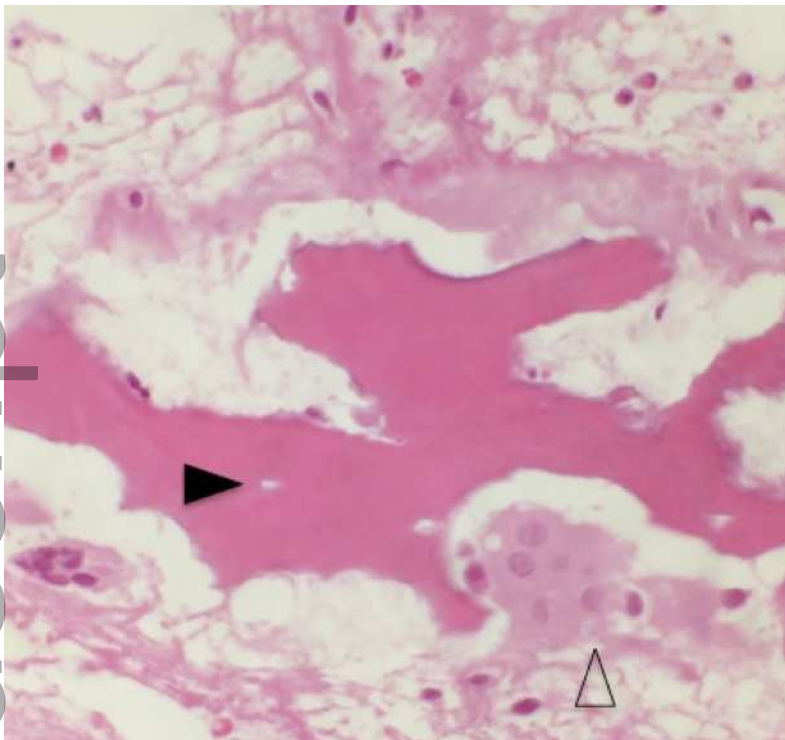


ara\_12796\_f2a.tiff

# Author Manuscript

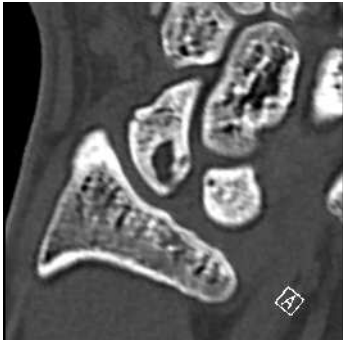


ara\_12796\_f2b.tiff



ara\_12796\_f2c.tiff

# Author Manuscript



ara\_12796\_f3a.tiff



ara\_12796\_f3b.tiff

# Author Manuscript



ara\_12796\_f3c.tiff

# Author Manuscript

# Author Manuscript



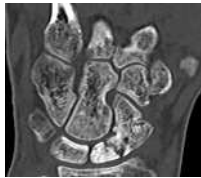
ara\_12796\_f4a.tif

# Author Manuscript



ara\_12796\_f4b.tif

# Author Manuscript



ara\_12796\_f4c.tif